Stimulation of the caudal zona incerta is superior to stimulation of the subthalamic nucleus in improving contralateral parkinsonism

Puneet Plaha,[1] Y. Ben-Shlomo,[2] Nikunj K. Patel[1] and Steven S. Gill[1]

[1]Institute of Neurosciences, Department of Neurosurgery, Frenchay Hospital and [2]Department of Social Medicine, University of Bristol, Bristol, UK

Correspondence to: Steven S. Gill, Frenchay Hospital, Bristol BS16 1LE, UK
E-mail: steven.gill@north-bristol.swest.nhs.uk

Deep brain stimulation (DBS) has an increasing role in the treatment of idiopathic Parkinson's disease. Although, the subthalamic nucleus (STN) is the commonly chosen target, a number of groups have reported that the most effective contact lies dorsal/dorsomedial to the STN (region of the pallidofugal fibres and the rostral zona incerta) or at the junction between the dorsal border of the STN and the latter. We analysed our outcome data from Parkinson's disease patients treated with DBS between April 2002 and June 2004. During this period we moved our target from the STN to the region dorsomedial/medial to it and subsequently targeted the caudal part of the zona incerta nucleus (cZI). We present a comparison of the motor outcomes between these three groups of patients with optimal contacts within the STN (group 1), dorsomedial/medial to the STN (group 2) and in the cZI nucleus (group 3). Thirty-five patients with Parkinson's disease underwent MRI directed implantation of 64 DBS leads into the STN (17), dorsomedial/medial to STN (20) and cZI (27). The primary outcome measure was the contralateral Unified Parkinson's Disease Rating Scale (UPDRS) motor score (off medication/off stimulation versus off medication/on stimulation) measured at follow-up (median time 6 months). The secondary outcome measures were the UPDRS III subscores of tremor, bradykinesia and rigidity. Dyskinesia score, L-dopa medication reduction and stimulation parameters were also recorded. The mean adjusted contralateral UPDRS III score with cZI stimulation was 3.1 (76% reduction) compared to 4.9 (61% reduction) in group 2 and 5.7 (55% reduction) in the STN (P-value for trend <0.001). There was a 93% improvement in tremor with cZI stimulation versus 86% in group 2 versus 61% in group 1 (P-value = 0.01). Adjusted 'off–on' rigidity scores were 1.0 for the cZI group (76% reduction), 2.0 for group 2 (52% reduction) and 2.1 for group 1 (50% reduction) (P-value for trend = 0.002). Bradykinesia was more markedly improved in the cZI group (65%) compared to group 2 (56%) or STN group (59%) (P-value for trend = 0.17). There were no statistically significant differences in the dyskinesia scores, L-dopa medication reduction and stimulation parameters between the three groups. Stimulation related complications were seen in some group 2 patients. High frequency stimulation of the cZI results in greater improvement in contralateral motor scores in Parkinson's disease patients than stimulation of the STN. We discuss the implications of this finding and the potential role played by the ZI in Parkinson's disease.

Introduction

Deep brain stimulation (DBS) has an increasing role in the treatment of medically refractory idiopathic Parkinson's disease. The subthalamic nucleus (STN) is the commonly chosen target and its dorsolateral part has been defined by

some groups as the optimal site for stimulation (Lanotte et al., 2002; Saint-Cyr et al., 2002; Yelnik et al., 2003; Herzog et al., 2004; Zonenshayn et al., 2004). Other groups, however, have reported that the most effective contact on a quadripolar DBS lead (Model 3389 or 3387, Medtronic Inc. Minneapolis) lies dorsal/dorsomedial to the STN in the region of the pallidofugal fibres and the rostral zona incerta (rZI) (Lanotte et al., 2002; Voges et al., 2002); and yet other groups have reported the optimal target as being at the junction between the dorsolateral part of the STN and the region dorsal/dorsomedial to it (Hamel et al., 2003; Herzog et al., 2004; Yokoyama et al., 2001).

The STN is a small biconvex-shaped nucleus measuring ∼9 × 7 × 4 mm (length × height × breadth) (Schaltenbrand and Wahren, 1977; Morel et al., 1997). Its anterior and lateral surface is surrounded by myelinated fibres of the internal capsule. The pallidofugal fibres crossing the internal capsule pass over the dorsal and medial surfaces of the STN, separating it from the dorsomedially placed rZI and more medially the prelemniscal radiation and the red nucleus. Lying posterior to the STN is the caudal or motor component of the zona incerta nucleus (cZI), which extends behind the prelemniscal radiation. Ventral to the zona incerta is the substantia nigra (Schaltenbrand and Wahren, 1977; Yelnik and Percheron, 1979; Parent and Hazrati, 1995).

The combined length from the tip of the DBS lead to the uppermost platinum/iridium contact varies from 9.00 mm (Model 3389, Medtronic Inc., Minneapolis, MN, USA) to 12.00 mm (Model 3387 Medtronic Inc.). Following the implantation of a DBS lead into the STN, the quadripolar lead transfixing it will have at least one or possibly two contacts lying either dorsal or dorsomedial to the STN in the region of the pallidofugal fibres and the rZI while the rest will lie within the nucleus. The therapeutic benefit seen following stimulation through any of the four contacts could therefore be due to stimulation of one or more structures that may influence the symptoms of Parkinson's disease. In addition to the anti-parkinsonian effect of stimulating the STN, benefit may be gained by including the pallidofugal fibres in the stimulation field. Lesions involving the zona incerta have also been reported as improving all three cardinal signs of Parkinson's disease (Houdart et al., 1965; Mundinger, 1965). In our own series of patients who underwent a subthalamotomy for Parkinson's disease, we found that a lesion involving the ZI produced a greater clinical benefit than one confined to the STN (Patel et al., 2003a).

In order to define the anatomical location of each contact on the DBS lead we used a novel MRI directed method (discussed in detail later) (Patel et al., 2002; Plaha et al., 2004). We analysed our outcome data on patients who underwent STN DBS surgery for Parkinson's disease between April 2002 and June 2003; the chosen target was the dorsal half of the STN at the junction of its anterior two-thirds and posterior one-third. We observed that the coronal axis of the STN varied from 15° to 57° from the sagittal plane. Where

the coronal axis was more vertical, the active contact was the same as the planned contact in the dorsal part of the STN. With a more horizontally located STN, the active contact was the one located dorsomedial/medial to the STN, involving the pallidofugal fibres and the rZI, rather than the planned contact in the dorsal STN (Fig. 1). This latter group had a better outcome than in those where the active contact was confined to the STN.

Subsequently, between June 2003 and August 2003, we specifically targeted the pallidofugal fibres and rZI, dorsomedial/medial to the STN. A few patients in this group suffered speech deterioration with optimal therapeutic stimulation. We found that in some of these patients stimulation of deeper and more posterior contacts on the lead (implanted at a 45° angle to the AC/PC plane) that encroached on the cZI maintained therapeutic benefit but avoided speech disturbance. Hence, from September 2003 onwards we have targeted posterior and medial to the STN in the cZI. In this manuscript, we now present a comparison of the motor outcomes between these three groups of patients with optimal DBS contacts within the postero-dorsal STN (group 1), dorsomedial/medial to the STN (group 2) and posterior to it within the cZI (group 3). We found that the contralateral motor score improvement was greater with cZI stimulation than with stimulation of the STN or medial/dorsomedial to it. We discuss the significance of these findings and how the cZI could be a potential target for DBS in Parkinson's disease.
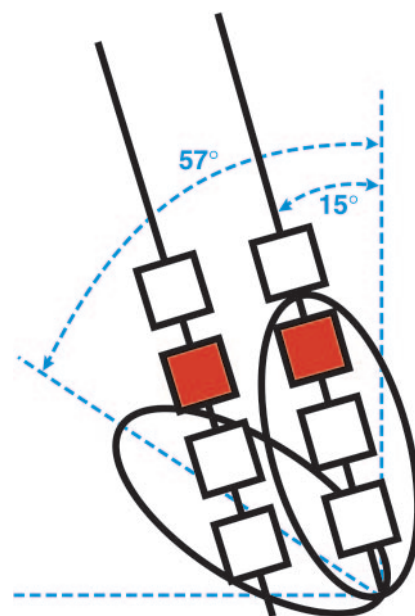

Fig. 1 Schematic line diagram showing the relationship of the active contact on the DBS lead to the STN in the coronal plane, depending on its long axis of rotation with respect to the mid-sagittal plane. Contacts shown in red colour were identified as active contacts.

Material and methods

Patient population

Thirty-five patients with medically refractory idiopathic Parkinson's disease as defined by the United Kingdom Parkinson's Disease Society brain bank criteria (Hughes *et al.*, 1992) were operated on between April 2002 and June 2004. There were 22 males and 13 females who together had a mean age of 60.5 years (SD 8.3 years). A total of 64 leads were implanted in the subthalamic region in these patients (29 patients had bilateral implants and 6 patients with predominantly unilateral symptoms had unilateral leads implanted). Every patient gave fully informed consent to have DBS leads implanted in a specific area of the subthalamic region (in the initial cohort of patients this was the STN, in the next group this was medial/dorsomedial to the STN and after that the cZI) and was aware of the potential risks of stereotactic surgery. The Frenchay hospital local ethical committee gave approval to perform stereotactic procedures under general anaesthesia using implantable guide tubes to deliver the DBS leads.

Clinical evaluation

Clinical evaluations were based on the Core Assessment Program for Surgical Interventional Therapies (CAPSIT), a validated protocol for evaluating surgical treatments of idiopathic Parkinson's disease and included the Unified Parkinson's Disease Rating Scale (UPDRS) and timed motor tests (Defer *et al.*, 1999). All patients were assessed by applying the Part III or the motor component of the UPDRS. A specialist movement disorder nurse performed the evaluations in all cases at baseline and 6 months (median value) following surgery.

Patients were assessed in the practically defined 'off' state, having stopped their anti-parkinsonian medications for at least 12 h overnight. Their 'on' state was assessed after giving patients a dose which was 1.25 times higher than their normal morning L-dopa dose plus equivalents of agonist. Post-surgery, they were assessed 12 h after stopping anti-parkinsonian medications and switching off the stimulation (off medication/off stimulation); and then 60–90 min after switching on the DBS (off medication/on stimulation). Dyskinesia was measured using the dyskinesia rating scale as part of the CAPSIT protocol (Defer *et al.*, 1999). This was assessed at baseline on medications and then at follow-up on medications/on stimulation.

Outcome measures

The primary outcome measure was the contralateral UPDRS III or motor UPDRS in the off medication/off stimulation state compared with the off medication/on stimulation state when measured at follow-up (excluding axial symptoms comprising speech, facial expression, gait, posture, postural stability and body bradykinesia i.e. Items 18, 19, 27–31). Secondary outcome measures included the UPDRS III subscores for tremor, rigidity and bradykinesia (finger taps, hand movements, rapid alternating movements of hands and leg agility). Timed hand movements, reduction in L-dopa equivalent dose, dyskinesia score, stimulation parameters and complications related both to the surgical procedure and post-operative stimulation were recorded.

Target definition

STN target: This was defined as being in the dorsal half of the STN at the junction of its anterior two-third and posterior one-third.

Dorsomedial/medial to STN: This target was defined as being outside the STN and medial/dorsomedial to the junction of its anterior two-thirds and posterior one-third.

Caudal zona incerta: The caudal or motor ZI was defined as being posteromedial to the postero-dorsal STN.

MR imaging and target planning

Under general anaesthesia, a modified Leksell stereotactic frame (it has non-conducting plastic posts and is fixed to the skull using carbon fibre pins inserted into drill holes made in the outer table) was fixed parallel to the orbito-meatal plane. Patients then underwent high resolution MRI T2 scan sequences (1.5 tesla imager, TR 2500 ms, TE 150, turbo-spin echo factor 11, number of signal averages 12, 512 × 512 matrix size, axial sequence of 15 slices for 18 min, coronal 15 slices for 18 min, sagittal 9 min and a total scan time of 45 mins) through the diencephalon to define the STN and the red nucleus. The anterior and posterior commissures (AC and PC) were identified in a mid-sagittal planning scan. Axial images 2 mm thick (voxel size 0.45 × 0.45 mm) were acquired parallel to the AC–PC plane and coronal images orthogonal to these were then obtained. Magnified hard copies (×1.6) of the T2 scans were obtained and overlaid on matched inverted T2 images, further to enhance definition of the STN and surrounding structures. The boundary of the STN, red nucleus and related structures were outlined on the inverted images. The defined boundaries in any one axial image were confirmed by cross correlating them with the boundaries on co-registered coronal and sagittal images. Likewise, boundaries defined on coronal images were cross-correlated with co-registered axial and sagittal images. The Schaltenbrand and Bailey atlas was used as a visual guide to assist in defining the anatomical structures in the subthalamic region (Schaltenbrand and Bailey, 1959). The target was then defined on the co-registered images in each of the three planes. Most typically, for the STN and cZI target, the middle of the second contact on the DBS lead (contact 1or 5) was placed at the target site, while for the target dorsomedial/medial to the STN, the middle of the third contact (contact 2 or 6) was placed at the target site. A transfrontal trajectory was planned that was 45° to the AC–PC plane and passed through the head of the caudate nucleus.

Surgery and target verification

Surgery was performed under general anaesthesia in a semi-sitting position, such that the frontal burr holes were uppermost. Before opening the dura and during the operative procedure the burr holes were continuously irrigated with normal saline to prevent air entry and consequent brain shift. A rigid tungsten probe of 1.27 mm diameter (equivalent to the diameter of a Medtronic 3389 and 3387 DBS lead) with a tapered and pointed end was inserted to the target, and over this a plastic guide tube was advanced so that the distal end of the plastic guide tube was short of the target by 12 mm. The guide tube is a thin walled tube (wall thickness of 0.1 mm) with a threaded cylindrical hub positioned at its proximal end. The hub has a dome shaped proximal end that is bisected by a slot that is in continuity with the bore of the guide tube. The proximal end of the guide tube was bonded within the burr hole with acrylic cement. The probe was then withdrawn and replaced with a relatively stiff plastic stylette (the plastic stylette has a T-shaped proximal end which fits within the hub of the guide tube) cut to an appropriate length, such that its distal end traversed the target to a planned position in the subthalamic region (Fig. 3A) (the
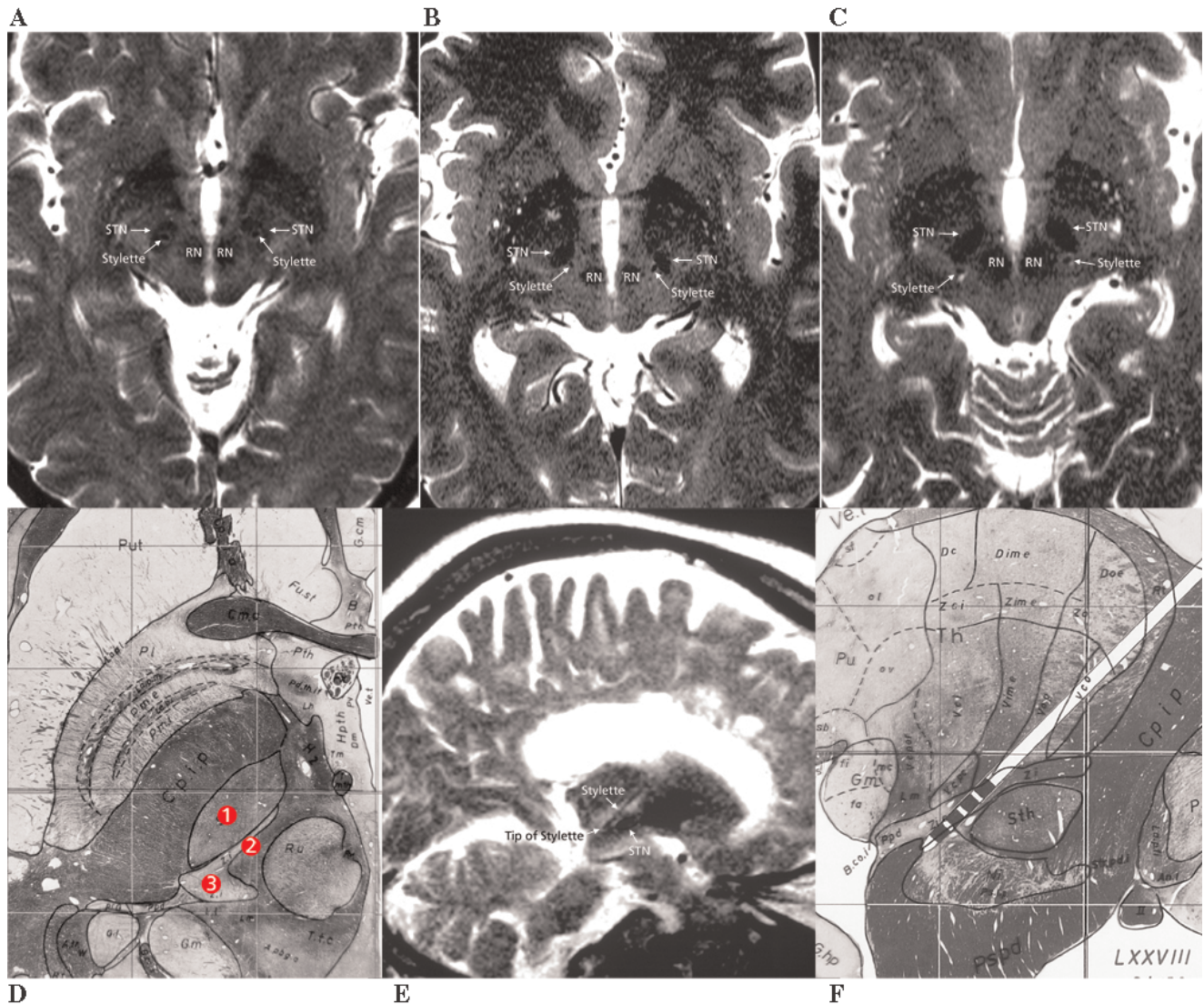
Fig. 2 Intra-operative axial MRI scan showing bilateral stylettes in the (**A**) STN, lateral to the anterior border of the red nucleus. (**B**) medial/dorsomedial to the STN and in the (**C**) caudal zona incerta (RN red nucleus, STN subthalamic nucleus). (**D**) Axial slice from the Schaltenbrand atlas showing the position of the three different subthalamic areas targeted. (**E**) Intra-operative sagittal MRI scan showing the transfrontal trajectory of the stylette passing dorsal to the outlined STN and its tip posterior to it in the caudal zona incerta. (**F**) Matching sagittal slice from the Schaltenbrand atlas with a DBS lead drawn to scale and the anatomical location of each contact on it.

guide tubes and stylettes are in-house investigational devices made of polycarbourethane and manufactured by Renishaw Plc, UK).

This procedure was carried out bilaterally except in six patients. Patients then underwent intra-operative MR scans to verify the position of the plastic stylette relative to the planned target (Fig. 2). Upon confirmation of satisfactory placement, the patient was returned to the operating theatre and the frame was removed. The plastic stylette was removed from the in-dwelling guide tube and measured off against the DBS lead (Model 3389, Medtronic Inc.). A suture was tied around the lead at the measured length. Once inserted the DBS lead's tungsten guide wire was removed and the lead bent through a 90° arc conforming with that within the slotted hub of the guide tube. When the suture on the DBS lead came into contact with the hub of the guide tube, the tip of the DBS lead was at the same subthalamic location as that of the stylette.

This also allowed us to establish the exact anatomical position of each of the four contacts in the subthalamic region (Fig. 3B). Each lead was then secured to the skull with an inverted U-shaped mini-plate and screws, connected to an extension cable and thence to the DBS pulse generator (Kinetra, Medtronic Inc., Minneapolis, MN). The pulse generator was implanted in a subcutaneous pocket below the clavicle. The whole procedure typically took $3\frac{1}{2}$–4 h, including intra-operative imaging and implantation of the DBS device.

Accuracy of guide tube DBS delivery
To calculate the accuracy of guide tube placement as planned, the intra-operative MRI scan was overlaid on to the plan pre-operative inverted MRI image. Using this technique, the two images subtracted except for the target marked on the plan scan and
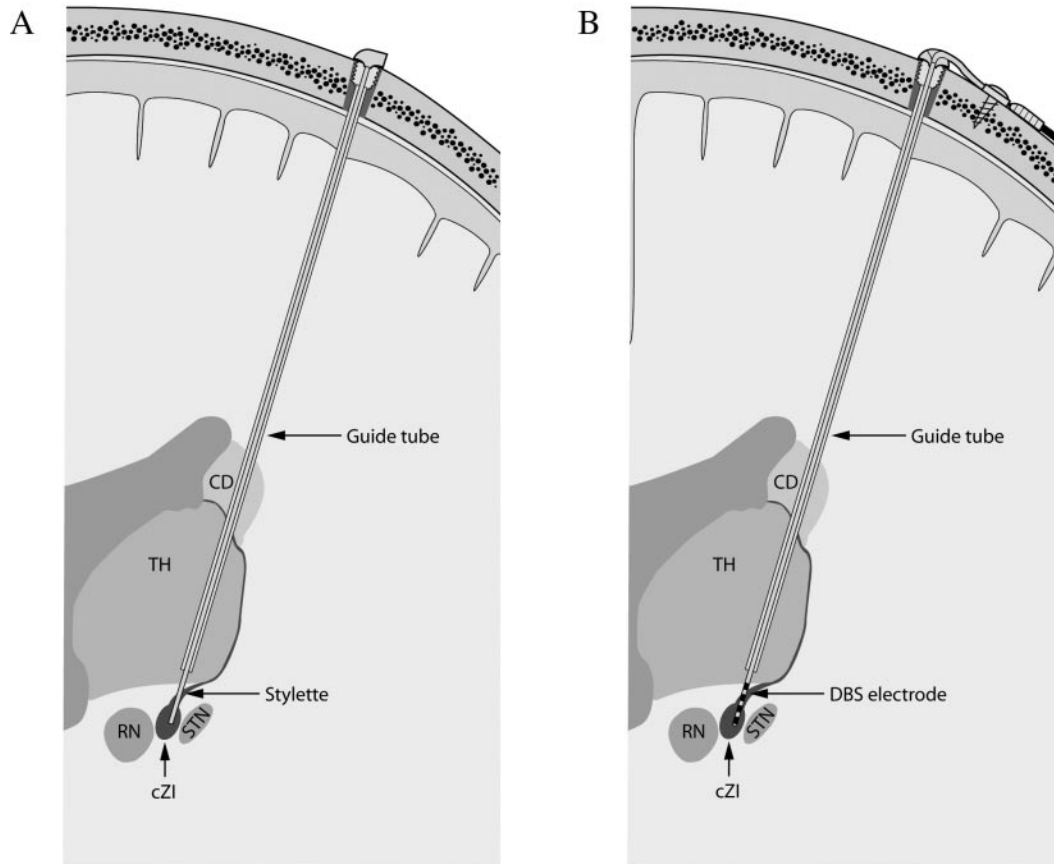
Fig. 3 (**A**) Line diagram drawn to scale, showing the intra-operative position of the guide tube and stylette in the caudal zona incerta. (**B**) Line diagram drawn to the same scale as in **A**; the stylette has been removed and replaced with the DBS lead to the same depth. Also note the guide tube is cut short of the target and therefore all four DBS contacts are exposed. The anatomical location of each contact on the DBS lead can therefore be determined (RN, red nucleus; cZI, caudal zona incerta; STN, subthalamic nucleus; TH, thalamus; CD, head of caudate nucleus).

the stylette visualized on the intra-operative scan. The displacement of the mid-point of the stylette with reference to the mid-point of the planned target in the mediolateral and anteroposterior plane was then measured. A displacement of the stylette by >1.5 mm from the planned target was deemed suboptimal and the subcortical nucleus was re-targeted and its accuracy confirmed on a repeat intra-operative MRI scan.

Post-operative management

Patients were programmed post-surgery by the movement disorder nurse who was guided by both the neurosurgeon and the neurologist. The best therapeutic DBS contact was identified and L-dopa medications were reduced as appropriate on the advice of the neurologist.

Anatomical location of active contacts

The active contact programmed on the DBS lead was noted. Its anatomical location was identified by superimposing the intra-operative MRI scan onto the pre-operative MRI plan scan on which we had defined the anatomical location of each DBS lead contact. The coordinates of the active contact were measured with respect to the inter-commissural point. Where monopolar

stimulation was used, the coordinates were measured from the middle of the contact. Where bipolar stimulation was used, the coordinates were measured from the middle of the contact acting as the cathode (Holsheimer, 2003).

In addition, we also defined the spatial location of the active contact in relation to the borders of the STN for all three target groups and transposed these positions into the Schaltenbrand and Bailey atlas. For an active contact within the STN, as identified from the intra-operative MRI plan scan, we first defined its intra-STN vertical location by measuring its distance from the dorsal most boundary of the STN at its mid-point. We then chose the appropriate intra-operative axial MRI slice to define its anteroposterior position as a proportion of the length of the STN along its axis. We also defined the mediolateral position as a proportion of the width of the STN in a plane orthogonal to the long axis. This technique defined the spatial location of the active contact within the STN.

We then transposed this spatial location into the STN identified on the Schaltenbrand and Bailey atlas by proportional measurements. For active contacts outside the STN, i.e. dorsomedial/medial to it or in the cZI, their spatial location was defined in relation to the adjacent borders of the STN. These were similarly transposed onto the Scahltenbrand and Bailey atlas.

Statistical analysis

For most of the outcome variables, we used linear regression analysis to compare differences in off medication/on stimulation absolute scores by procedure. This was adjusted for off medication/off stimulation scores at follow-up, as a measure of disease severity, sex and age group (<55 years, 55–64 years, greater and equal to 65 years) with the STN patients as the reference group. Because most patients had more than one DBS lead implanted (29 bilateral implants and 6 unilateral implants), we used robust standard errors to take into account the clustered nature of the data; this approach is more conservative than standard methods and results in slightly wider confidence intervals and hence larger *P* values.

We present both the crude and adjusted absolute scores by procedure and *P* values. We have also converted the absolute change in scores to a relative percentage improvement and 95% confidence interval, by dividing this value by the STN off medication/off stimulation value and multiplying by 100. The proportion of subjects whose dyskinesia score improved (binary variable) was modelled using generalized linear models. Fifteen subjects were omitted from the analysis of the tremor score as their off medication/off stimulation tremor score was zero and they could not show improvement. We also used the cZI rather than the STN group as the baseline for the percentage improvement in tremor as the adjusted improvement for the cZI group would have resulted in a >100% improvement due to the milder off medication/off stimulation scores for the STN group. We carried out a sensitivity analysis on our data to see if this altered our qualitative interpretation. We repeated the above analyses using the baseline off scores, rather than off medication/off stimulation scores at follow-up.

Results

Seventeen DBS leads were identified with the best therapeutic contact in the STN, 20 with active contacts dorsomedial/medial to STN (involving pallidofugal fibres and rZI) and 27 with contacts in the cZI. In the 6 unilaterally implanted patients, 2 contacts were in the STN, 3 dorsomedial/medial to it and 1 in cZI. Table 1 shows the data for follow-up both in absolute and relative terms. We have presented both the crude and statistically adjusted mean values so that the reader can see how adjustment alters the results. The absolute improvement in scores can be calculated by simply subtracting the off/off scores from the off/on scores.

Contralateral UPDRS III score (Table 1)

The contralateral UPDRS III score following stimulation was best in the cZI group (3.1), followed by the group dorsomedial/medial to the STN (4.9) and then the STN group (5.7). This was equivalent to a 76, 61 and 55% relative reduction in score respectively (*P*-value for trend <0.001)

Contralateral tremor score (Table 1)

The contralateral tremor score showed a very marked reduction for the cZI from 4.29 to 0.29, whilst the STN group improved more modestly from 2.31 to 1.66, after adjustment. In relative terms, the STN group improved by 61% (95% CI 37–85%), compared to 86% (95% CI 73–98%) in the group dorsomedial/medial to the STN and 93% in the cZI group.

Whilst the trend could have been due to chance, the difference in improvement between the STN and cZI group is unlikely to be due to chance (*P* = 0.01).

Contralateral rigidity score (Table 1)

The contralateral upper and lower limb rigidity scores following stimulation were very similar for both STN and the group dorsomedial/medial to the STN, but was over 1 point less for the cZI group (*P* = 0.003). This was equivalent to a 76% (95% CI 60–93%) relative improvement in the cZI group as compared to 50% in the STN group and 52% (95% CI 32–72%) in the group dorsomedial/medial to the STN.

Contralateral bradykinesia score (Table 1)

The bradykinesia score following stimulation improved by 59% in the STN group compared to 56% (95% CI 40–72%) in the group dorsomedial/medial to the STN and 65% (95% CI 54–75%) in the cZI group but may have been due to chance (*P*-value for trend = 0.17)

Contralateral timed hand movements (Table 1)

The contralateral timed hand movements improved by 25% in the STN group compared to 33% (95% CI 24–40%) in the group dorsomedial/medial to the STN and 45% (95% CI 39–52%) in the cZI group. The *P*-value for improvement in cZI compared to the STN was <0.001.

Dyskinesia score and L-dopa medications (Table 1)

Maximal reduction in dyskinesia scores was seen in the group with active contacts dorsomedial/medial to STN (63%; 95% CI 32–93%), while in the STN group dyskinesia reduced by 41% compared to 56% (95% CI 21–91%) in the cZI group, but these differences may have been due to chance. Similarly, differences in L-dopa medication may have occurred by chance (*P*-value for trend = 0.11).

Pulse generator parameters (Table 1)

There was no statistical difference between the three groups in the stimulation parameters of voltage, pulse width and frequency of stimulation.

Sensitivity analysis

We repeated all the above analyses adjusting for the baseline 'off' medication scores rather than the follow-up off medication/off stimulation scores. This did not alter the qualitative pattern of results but produced slightly larger *P* values (Supplementary Table 1). For example, the relative improvement for the cZI group was now 75% (95% CI 58–90), *P*-value = 0.02, compared to 55% in the STN group and the *P*-value for trend was 0.008. The revised *P* values for trend were accordingly: 0.05 for tremor, 0.006 for rigidity, <0.001 for the timed hand movements.

Table 1 Mean motor scores at follow-up 'off' all medications with the stimulator switched off ('off-off') compared to 'off' medications with the stimulator switched 'on' ('off-on') in three different anatomical locations

Location of DBS	STN	Medial to STN	Caudal ZI	P-value for trend
No of DBS leads	17	20	27	
Contralateral UPDRS III				
Crude off/off score (Mean)	12.7	13.8	15.7	
Crude off/on score (Mean)	5.7	5.4	4.4	
Adjusted off/on score (Mean)	5.7	4.9	3.1	
Adjusted per cent improvement (95% CI)[†]	55%	61% (46–76)	76% (65–87)	
P-value		0.42	<0.001	<0.001
Contralateral tremor[††]				
Crude off/off score (Mean)	2.31	3.27	4.29	
Crude off/on score (Mean)	1.08	0.33	0.29	
Adjusted off/on score (Mean)	1.66	0.63	0.29	
Adjusted per cent improvement (95% CI)[†]	61% (37–85)	86% (73–98)	93%	
P-value	0.01	0.19		0.21
Contralateral rigidity				
Crude off/off score (Mean)	4.2	4.1	4.3	
Crude off/on score (Mean)	2.1	2.0	1.1	
Adjusted off/on score (Mean)	2.1	2.0	1.0	
Adjusted per cent improvement (95% CI)[†]	50%	52% (32–72)	76% (60–93)	
P-value		0.86	0.003	0.002
Contralateral Bradykinesia				
Crude off/off score (Mean)	6.8	7.3	8.1	
Crude off/on score (Mean)	2.8	3.2	3.1	
Adjusted off/on score (Mean)	2.8	3.0	2.4	
Adjusted per cent improvement (95% CI)[†]	59%	56% (40–72)	65% (54–75)	
P-value		0.74	0.28	0.17
Timed hand movements (s)				
Crude off/off time in sec (Mean)[‡]	13.7	13.5	16.0	
Crude off/on time in sec (Mean)[‡]	10.3	9.0	7.9	
Adjusted off/on score (Mean)	10.3	9.2	7.5	
Adjusted per cent improvement (95% CI)[†]	25%	33% (24–40)	45% (39–52)	
P-value		0.08	<0.001	<0.001
Dyskinesia scores on medication*				
Crude percentage improvement	41	65	56	
Adjusted percentage improvement (95% CI)[†]	41%	63% (32–93)	56% (21–91)	
P-value		0.16	0.40	0.56
L-Dopa equivalent medication (mg)				
Pre-op (mean)	1152	918	1130	
Post-op (mean)	631	542	764	
Adjusted per cent improvement (95% CI)[§]	45%	47% (32–61)	32% (14–50)	
P-value		0.98	0.18	0.11
Stimulation parameters				
Voltage (mean)	2.65	2.49	2.71	
P-value		0.54	0.83	
Pulse width (mean)	81.2	84.0	82.2	
P-value		0.63	0.83	
Frequency (mean)	160.6	150.5	149.6	
P-value		0.21	0.17	

Also shown are the improvement in dyskinesia scores, L-dopa medication reduction and the stimulation parameters.
[†]Adjusted for sex, age group, off-off score and clustering; [††]ZI group taken as baseline and 15 patients omitted as their 'off/off' score was zero and they could not show improvement; [‡]geometric mean; *dyskinesia was scored as per CAPSIT protocol;
[§]adjusted for sex, age group, baseline medication dosage and clustering.

Accuracy of guide tube DBS delivery

In total, 65 guide tubes and stylettes were implanted and 65 DBS leads inserted through them in the 35 patients. Of the guide tube stylettes and subsequently the DBS leads, 93.75% were located within 1 mm of the planned target in the mediolateral plane and 95.31% within 1 mm of the target in the anteroposterior plane. Of the DBS leads, 100% were within 1.5 mm of the planned target. None of the

guide tube stylettes required re-positioning following the intra-operative MRI scan and all DBS leads were implanted on the first pass.

Coordinates of active contacts (Fig. 4)

Our STN target was planned in the dorsal half of the junction of the anterior two-thirds and posterior one-third with a
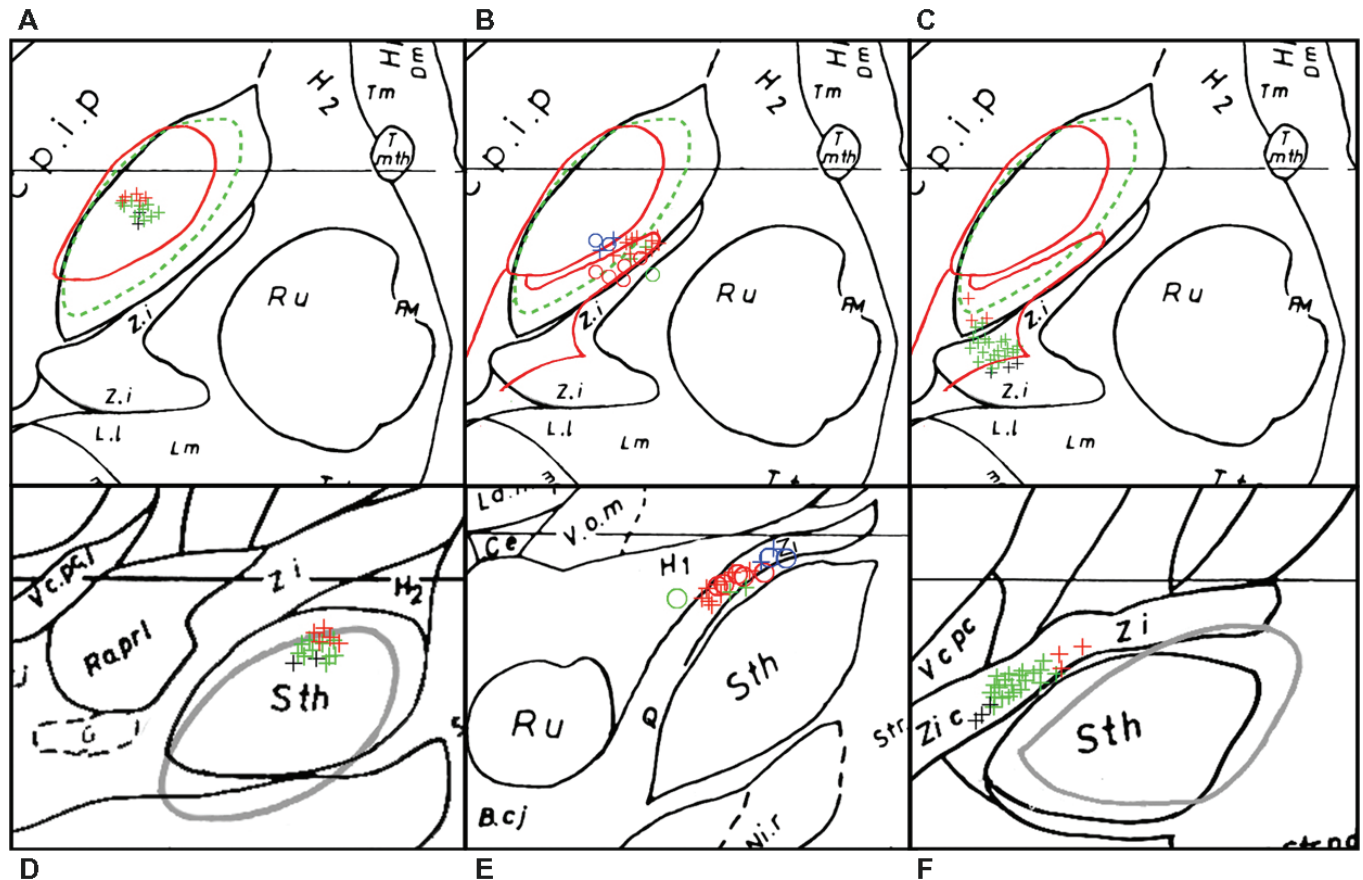
Fig. 4 Shows the spatial location of the active contacts in all three groups as transposed onto the Schaltenbrand atlas. (**A**) Active contacts in the STN (**B**) medial/dorsomedial to the STN and (**C**) caudal zona incerta. The STN and zona incerta from axial slice H.v −1.5 (drawn in red) are superimposed onto axial slice H.v −3.5 (shown in black) and the STN on H.v −2.5 is drawn out in between the two (dotted green). Active contacts (shown as crosses or circles) positioned at/or within 1 mm dorsal to a defined axial plane are shown in the same colour. Active contacts shown, as circles as shown in **B**, were associated with stimulation related side effects including hypophonic speech and disequilibrium. Active contacts shown in blue, though appearing at the dorsomedial border of the STN on slice H.v −1.5, are in fact dorsomedial to it at a higher plane as seen in the coronal plane (**E**). **D** shows the active contacts in the STN in the sagittal plane between slice S.l 12.0 (black colour) and the STN from slice S.l 13 (grey colour). **E** shows the active contacts dorsomedial/medial to the STN in the coronal plane with respect to slice F. P −3.0. **F** shows the active contacts in the caudal ZI between sagittal plane S.l 13.5 (grey colour STN) and S.l 15.0 (black colour).

45° transfrontal trajectory, and we placed the middle of the second contact (contact 1 or 5) at this target point. The optimal contact was either the second contact (contact 1 or 5) or more typically the third contact (contact 2 or 6) for monopolar stimulation or where bipolar stimulation was performed, in the majority of cases; the polarity favoured the proximal contact (contact 2 or 6). The mean position of the 17 active STN contacts was thus anterodorsal to our planned target and the coordinates were 12.4 ± 1.2 mm lateral to the AC–PC line in the mid-sagittal plane, 2.1 ± 1.3 mm posterior to the inter-commissural point and 2.3 ± 0.81 mm below the AC–PC plane. The active contacts in group 2 (dorsomedial/medial to the STN) were 11.37 ± 1.1 mm (x), −3.01 ± 0.8 mm(y) and −2.06 ± 0.9 mm (z) with respect to the inter-commissural point. The active contacts in cZI were 14.01 ± 1.56 mm (x), −5.8 ± 1.49 mm (y) and −2.1 ± 1.05 mm (z) with respect to the intercommissural point. The distribution

of the active contacts transposed onto the Schaltenbrand and Bailey atlas is shown in Fig. 4.

Complications (Fig. 6)

There were no peri-operative surgical complications in any of the three groups. During this follow-up period there were no device related complications. Side effects at optimal stimulation were seen in four patients in group 2 (active contacts dorsomedial/medial to the STN). Unilateral stimulation of the active contacts in these four patients resulted in no side effects however, bilateral stimulation resulted in reversible, hypophonic, slurred speech and a sense of disequilibrium when walking. The anatomical location of some, as analysed by superimposing the intra-operative MRI scan on to the pre-operative MRI plan scan, was found to be more medially placed and encroaching on the preleminiscal radiation (see Fig. 4B and 4E).

Discussion

This observational study indicates that the cZI is superior to the STN in improving contralateral motor scores for the treatment of medically refractory Parkinson's disease while bilateral stimulation medial/dorsomedial to the STN is associated with speech and balance problems.

Target definition on MRI

Using our imaging sequence, deep brain targets are defined on long acquisition, high-resolution MR images acquired through the diencephalon under strict stereotactic conditions, in the axial, coronal and sagittal planes with a slice thickness of 2 mm and voxel size 0.45×0.45 mm. Repeated long acquisition (total scan time of 45 min) of the 2 mm slice volume increases the signal-to-noise ratio and maintains the optimal balance between the image sensitivity and high spatial resolution. Frame related artefact is minimized by using our modified Leksell stereotactic frame, with non-conducting plastic posts, and any movement related artefact is minimized by imaging under general anaesthesia with the head frame fixed within the head coil.

The STN, red nucleus and the mammillo-thalamic tract are well visualized on the MRI images. The visibility and boundaries of the STN target may be increased by adjusting the window setting of the T2-weighted images maximizing the grey/white matter contrast and by using magnified hard copy images. The boundaries may be enhanced by overlaying inverted images on to standard T2 images, a method which neutralizes the grey areas and allows for easier identification of the bright STN edges on a dark background. Cross-correlation of STN in axial, coronal and sagittal planes, a process that takes several hours and constructs a 3D map of the target, is a very useful method as boundaries poorly seen in one plane are often better seen on another plane. The high signal area of the internal capsule is also very useful in defining the lateral and posterior boundary of the STN. All these methods are especially useful when the posterior dorsolateral portion of the STN is sometimes seen as a patchy hypointense area on the coronal images rather than a discrete hypointense signal like the posteroventral part due to a decrease in iron content in this part of the nucleus in patients with Parkinson's disease (Kosta *et al.*, 2006).

Guide tube technique

This technique provides a means of confirming the accuracy of targeting using intra-operative MR imaging to identify the relationship of an indwelling stylette to the visualized anatomical target (Patel *et al.*, 2002; Plaha *et al.*, 2004). The technique also enables the surgeon to identify the precise anatomical location of each contact on the DBS lead. This is because the stylette is replaced with the DBS lead to exactly the same length and is inserted down the bore of the fixed guide tube. As the DBS lead is of the same width as the bore of the guide tube, it fits snugly when inserted down the bore and will not move within the brain. The DBS lead is only unprotected for the last 12 mm of its path to the target, but will not move as the bore of the guide tube will guide it straight to the target. Also, with the guide tube secured with acrylic cement to the burr hole there is no movement of the guide tube. Hence when the DBS lead is secured to the skull bone after being bent through right angles within the slot in the hub of the guide tube, there can be no movement of the tip of the DBS lead.

Our method contrasts with the use of post-operative MRI to identify the anatomical position of each contact, where image artefact due to the metal in the lead makes accurate localization unreliable and in addition may carry some risk to the patient (Rezai *et al.*, 2004). Indirect methods of contact localization have also been described which include the use of intra-operative microelectrode recording to define the boundaries of the STN (Saint-Cyr *et al.*, 2002; Hamel *et al.*, 2003; Herzog *et al.*, 2004; Zonenshayn *et al.*, 2004). These methods, however, will not provide sufficient anatomical detail to be certain where each contact lies in relationship to the STN volume and will not account for brain shift occurring between removal of the microelectrode and insertion of the larger DBS lead.

Anatomical location of the active contact

In this study, the mean anatomical location of the active contact in each of our three groups was defined in relation to the inter-commissural point and projected onto the Schaltenbrand and Bailey atlas. In this way, their positions could be compared with the mean active contact positions in subthalamic region targets defined by other groups. Figure 5 shows that our mean STN active contact is in the dorsal STN region and lies lateral to the anterior border of the red nucleus, in a comparable location to other groups (Lanotte *et al.*, 2002; Saint-Cyr *et al.*, 2002; Hamel *et al.*, 2003; Herzog *et al.*, 2004). The cZI target lies posteromedial to the posterodorsal STN. Velasco *et al.* (2001) have implanted unilateral DBS electrodes into the posterior subthalamic region in the prelemniscal radiation, which is more medial and deeper than our cZI target. The prelemniscal radiation lies between the medial border of the STN and the lateral border of the red nucleus, with its posterior extent limited by the cZI and the posteromedially placed medial lemniscus (Schaltenbrand and Wahren, 1977). Recently, Kitagawa *et al.* (2005) have implanted unilateral DBS leads into the ZI/prelemniscal radiation and their target lies between our target and the target defined by Velasco *et al.* (2001) (see Fig. 5).

In order to evaluate the effective treatment volume and contact scatter within each anatomical target location, as well as to localize contacts producing side effects, we also defined the spatial location of each active contact with respect to the boundary of its relevant STN. The spatial location of all 64 active contacts was then transposed onto a standardized STN as defined on the Schaltenbrand and Bailey atlas (Fig. 4). This is a more useful method than using the
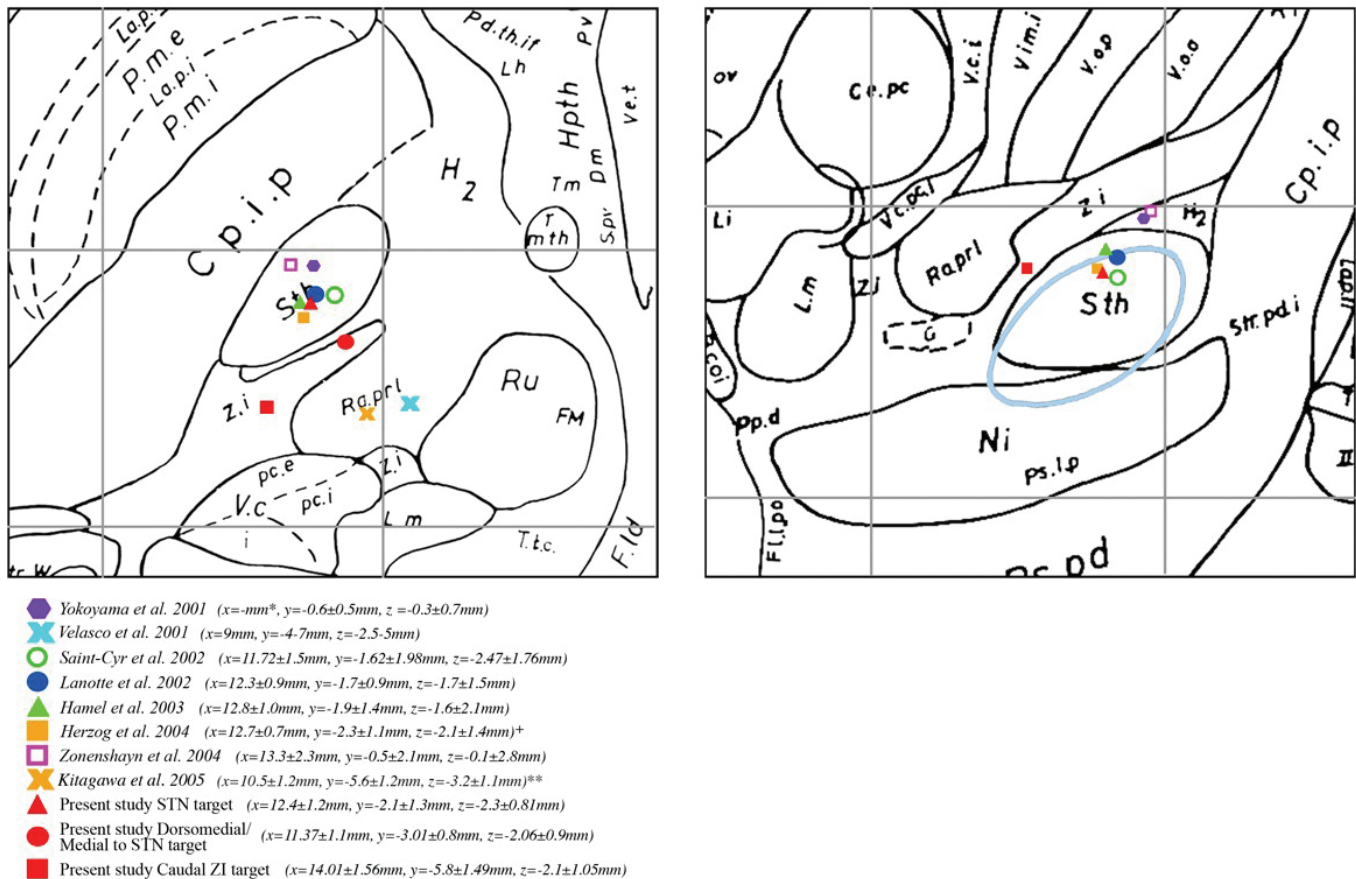
● Yokoyama et al. 2001 (x=-mm*, y=-0.6±0.5mm, z =-0.3±0.7mm)

✕ Velasco et al. 2001 (x=9mm, y=-4-7mm, z=-2.5-5mm)

○ Saint-Cyr et al. 2002 (x=11.72±1.5mm, y=-1.62±1.98mm, z=-2.47±1.76mm)

● Lanotte et al. 2002 (x=12.3±0.9mm, y=-1.7±0.9mm, z=-1.7±1.5mm)

▲ Hamel et al. 2003 (x=12.8±1.0mm, y=-1.9±1.4mm, z=-1.6±2.1mm)

■ Herzog et al. 2004 (x=12.7±0.7mm, y=-2.3±1.1mm, z=-2.1±1.4mm)+

□ Zonenshayn et al. 2004 (x=13.3±2.3mm, y=-0.5±2.1mm, z=-0.1±2.8mm)

✕ Kitagawa et al. 2005 (x=10.5±1.2mm, y=-5.6±1.2mm, z=-3.2±1.1mm)**

▲ Present study STN target (x=12.4±1.2mm, y=-2.1±1.3mm, z=-2.3±0.81mm)

● Present study Dorsomedial/Medial to STN target (x=11.37±1.1mm, y=-3.01±0.8mm, z=-2.06±0.9mm)

■ Present study Caudal ZI target (x=14.01±1.56mm, y=-5.8±1.49mm, z=-2.1±1.05mm)

Fig. 5 Mean value of the active contacts as defined by a number of groups in relation to the inter-commissural point, plotted onto the Schaltenbrand atlas in both the axial (figure on the left) and sagittal plane (figure on right). Axial plane H.v −1.5 is chosen, as the mean z coordinate of most of the groups is around 1.5 mm below AC–PC plane. In the sagittal plane, on the Schaltenbrand atlas, active contacts are plotted in relation to plane S.l 12 (black colour, STN) and the superimposed slice S.l 13 (light blue colour, STN). These two planes are chosen as the mean x coordinate of most groups is around 12–13 mm from the mid-sagittal plane. *x-value not given by the authors, but taken to be between 12–13 mm. + Values chosen are those of the junctional contacts which produced the best clinical outcome. **Although the z plane is deeper, x and y, coordinates plotted onto H.v −1.5 only for comparison with other groups.

inter-commissural point as the reference, given the significant intra- and inter-individual variation in the relationship of the inter-commissural point with the STN (Littlechild *et al.*, 2003; Patel *et al.*, 2003*b*; Richter *et al.*, 2004).

Patient outcome

In this study, we quantified therapeutic outcome using contralateral motor scores rather than the total UPDRS III motor score. This is because in patients undergoing implantation of DBS electrodes into the STN, the optimal contact on one side may lie within the STN, whilst on the other it may lie outside it. Therefore, in order to establish which target location is most efficacious, the investigator needs to assess contralateral motor scores for each contact location. This necessarily excludes axial scores, which result from the combined effect of stimulating both sides.

Although it is more conventional to compare the baseline 'off' medication scores with the follow-up off medication/on

stimulation score, we believe that our chosen comparison of comparing the follow-up off medication/off stimulation score versus the off medication/on stimulation score is more useful due to reduced measurement error. There may be up to a 15% variation between consecutive assessments on applying the UPDRS score, due to day-to-day variations in the patient's clinical condition. Thus, by comparing the off medication/off stimulation score with the off medication/on stimulation score at follow-up, this intra-individual variation will be minimized and a more precise estimate of the effects of stimulation will be obtained. Additionally, if there is variable disease progression and the time between baseline and follow-up visits is not the same for all patients, then two patients with similar baseline measures may have very different off-off scores regardless of the effectiveness of the therapy.

We do not believe that this approach has altered our conclusions as when we repeated our analysis comparing off medication/on stimulation scores with baseline 'off'

scores, the results were almost the same although, as might be expected, the 95% confidence intervals and *P* values were slightly larger for the reasons given above.

The reduction in the contralateral UPDRS III score for cZI compared to the baseline STN score was 75% (95% CI 58–90%, *P* = 0.02, *P*-value for trend = 0.008) rather than 76%; the improvement in rigidity in the cZI group was 77% (95% CI 56–98%, *P* = 0.02, *P*-value for trend = 0.006) rather than

Fig. 6 Schematic diagram of the subthalamic region, not drawn to scale. It shows the area in the caudal zona incerta where best clinical improvement was noticed and also the region in the prelemniscal radiation where some patients developed stimulation related speech and balance disturbance (cZI, caudal zona incerta).

76%; the improvement in timed hand movements was now 56% (95% CI 49–62%, *P* < 0.001, *P*-value for trend <0.001) rather than 45%. The adjusted improvement for tremor in the STN group was 64% (95% CI 34–93%, *P* = 0.05, *P*-value for trend 0.05) rather than 61%.

We have compared our outcome data for each of our three target locations with the outcome data provided by other groups, who have targeted similar regions. The primary purpose of this was to determine whether the difference between our cZI and STN group could be explained by suboptimal targeting and outcome in our STN group. As previously discussed, the mean coordinate of our active contact in the STN was directly comparable to other groups and as we show in Table 2, so is our outcome data. The outcome from groups reporting bilateral STN stimulation using total UPDRS III motor scores falls within the 50–65% range of improvement (Limousin *et al.*, 1998; Volkmann *et al.*, 2001; Figueiras-Mendez *et al.*, 2002; Ostergaard *et al.*, 2002; Kleiner-Fisman *et al.*, 2003; Krack *et al.*, 2003; Rodriguez-Oroz *et al.*, 2005). However, it is likely that the active contacts in these series would have included contacts within the STN, dorsal/dorsomedial to it or in other areas of the subthalamic region.

Groups who have correlated the anatomical location of the active contact with contralateral motor scores (Table 2) show that stimulation of the dorsal STN results in an improvement in contralateral motor scores by ≈50–63%, which is directly comparable to our outcome data of 55%. Although, as noted in the table, most of these group have compared baseline off scores with post-operative off/on scores.

Groups reporting on contralateral motor outcome with junctional contacts in the dorsal STN and rZI/pallidofugal fibres have reported improvement of ≈60% (Table 2). Voges
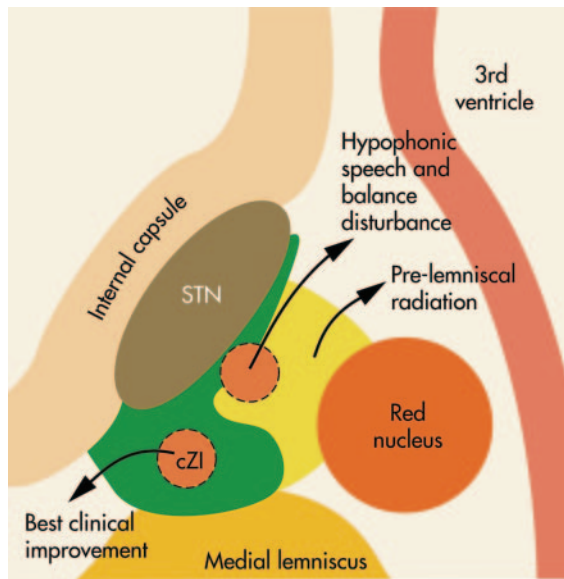
Table 2 Review table showing the anatomical location of the active contact with the contralateral motor outcome including subscores of tremor, rigidity and bradykinesia

Target	Authors	No. of electrodes	Follow-up (months)	Contralateral motor subscores improvement			Total contralateral motor improvement
				Tremor	Rigidity	Bradykinesia	
Dorsal STN	Saint-Cyr *et al.* (2002)	54	3	≈80%	≈42%	≈33%	50%*
	Voges *et al.* (2002)	3	14.4	–	–	–	≈64%*
	Herzog *et al.* (2004)	5	6	–	–	–	63.44 ± 22.6%**
	Present study	17	6	62% (37–86)	50%	59%	55%
Junctional including exclusively rZI/pallidofugal fibres	Yokoyama *et al.* (2001)	13	7–10 days	54.8 ± 32.8%	74.4 ± 20.4%	53.7 ± 14.3%	55.5%**
	Voges *et al.* (2002)	24	14.4	–	–	–	≈62–72%***
	Herzog *et al.* (2004)	15	6	–	–	–	65.3 ± 18.7%****
	Zonenshayn *et al.* (2004)	62	6	–	–	–	64 ± 17.9%**
	Present study	20	6	86% (73–98)	52% (32–72)	56% (40–72)	61% (46–76)
Caudal ZI/Prelemniscal radiation	Kitagawa *et al.* (2005)	8	24	78%	92.7%	65.7%	≈72%*****
Caudal ZI	Present study	27	6	93%	76% (60–93)	65% (54–75)	76% (65–87)

*% improvement calculated from baseline and post-operative median scores. **% improvement calculated from baseline and post-operative mean scores; ***≈62% improvement with junctional contacts at the interface of the dorsal STN and rZI/pallidofugal fibres and ≈72% with contacts exclusively in the rZI/pallidofugal fibres; ****junctional defined as being ± 1.5 mm from the dorsal border of the STN; *****% improvement calculated as the difference between the post-operative off/off score versus the off/on score.

et al. have reported ≈62% improvement with junctional contacts and where they subanalysed motor outcome data on active contacts exclusively in the rZI and pallidofugal fibres (6 DBS leads) there was an improvement of ≈72%. Our group 2 patients with contacts in the region of the rZI and pallidofugal fibres, including some more medially located leads that encroached on the prelemniscal radiation, showed an improvement of 61% (CI 46–76%).

Recently, Kitagawa *et al.* have performed unilateral stimulation in the region of the ZI and the prelemniscal radiation in patients with tremor-dominant Parkinson's disease with good improvement in contralateral motor subscores. They noted a 78.3% improvement in contralateral tremor, 92.7% improvement in rigidity and 65.7% improvement in contralateral bradykinesia with overall improvement in contralateral scores by ≈72%. Like us, they compared their patients off medication/off stimulation score at follow-up versus the off medication/on stimulation score to quantify outcome (Kitagawa *et al.*, 2005).

Active contacts in our group 2 patients showed a greater improvement in dyskinesia scores (65% reduction versus 41% in STN versus 56% in cZI) presumably because stimulation in this region involved the pallidofugal fibres and jammed the transmission of abnormal patterns of neuronal firing responsible for the expression of dyskinesia. There was no significant difference between the three groups in L-dopa equivalent medication reduction; however, the cZI group had a lesser medication reduction compared to the other groups. This probably reflected a trend in our practice to be less aggressive about medication reduction in view of the psychological effects that can be associated with a rapid levodopa withdrawal. Also, whether the slightly lesser reduction in medications in the cZI group compared to the STN group, coupled with a greater improvement in dyskinesia scores (41% in STN versus 56% in cZI), suggests an anti-dyskinetic effect of cZI stimulation is an interesting possibility.

We also considered the possibility that the difference in L-dopa responsiveness between the three groups could have accounted for the difference in motor outcome. We examined this possibility by comparing the differences in the outcome measures at baseline both off and on medication but found no statistically significant differences between any of the groups. The cZI group if anything showed marginally less levodopa responsiveness than the STN group. For example, the cZI group showed a reduction of 71.4% (95% CI 58.5–84.2%, $P = 0.60$) in the UPDRS III scores versus 74.8% in the STN group in response to a standardized L-dopa dose after adjustment for clustering, age group and sex.

There was no significant difference in stimulation parameters between the three groups.

Stimulation of the STN has been reported to be associated with a high incidence of neuropsychological complications (Berney *et al.*, 2002; Houeto *et al.*, 2002; Kulisevsky *et al.*, 2002). The caudal or motor ZI is posterior to the STN and away from the anterior limbic areas of the STN. It is therefore possible that DBS of the cZI may improve motor symptoms in Parkinson's disease without the associated neuropsychological sequel seen following STN stimulation, but this awaits further studies.

Complications

In total, we implanted 65 guide tube stylettes and subsequent DBS leads and none required repositioning as verified on the intra-operative MRI scan. There were no peri-operative complications, especially intra-operative haemorrhage. This was primarily because only one pass was required per target to implant the DBS lead in comparison to other techniques using microelectrode recordings where a greater number of passes increases the trauma to the brain and probably the risk of haemorrhage (Hariz and Fodstad, 1999; Binder *et al.*, 2005).

Stimulation related complications were seen in some group 2 patients who had more medially placed contacts. Four patients with bilateral contacts in this region developed a hypophonic speech and a sense of disequilibrium when walking. This we believe is due to spread of the stimulation current to the prelemniscal radiation—which contains cerebellar fibres and also fibres from the ascending mesencephalic reticular formation (Schaltenbrand and Wahren, 1977; Jimenez *et al.*, 2000). This is in contrast to the more usual explanation for stimulation related dysarthria, which is often attributed to spread of current to the motor limb of the internal capsule. Spread of the stimulation current to the cerebellar fibres which control the fine movements of the vocal cords is likely to cause a hypophonic speech while spread of current to proprioceptive fibres in the ascending mesencephalic reticular formation would account for the sense of disequilibrium while walking. The prelemniscal radiation has been lesioned (Ito, 1975) and stimulated (Velasco *et al.*, 2001) in the past. Velasco *et al.* reported improvement in tremor and rigidity but not bradykinesia scores. Three out of ten patients in their series developed stimulation related dysarthria and disequilibrium, which is consistent with our findings.

Zona incerta and its potential role in Parkinson's disease

The ZI, an embryological derivative of the ventral thalamus, is a distinct heterogeneous nucleus that lies at the base of the dorsal thalamus (Jones, 1985). It is divided into four sectors (rostral, dorsal, ventral and caudal). The rostral component extends over the dorsal and medial surface of the STN whilst its caudal or motor component lies posteromedial to the STN (Mitrofanis, 2004, 2005).

The ZI receives afferents from the basal ganglia output nuclei (globus pallidus internus and substantia nigra reticulata) (Roger and Cadusseau, 1985; Shammah-Lagnado *et al.*, 1985; Kolmac *et al.*, 1998; Heise and

Mitrofanis, 2004), the ascending reticular activating system (Watanabe and Kawana, 1982; Roger and Cadusseau, 1985; Shammah-Lagnado *et al.*, 1985; Kolmac *et al.*, 1998) and also motor, associative and limbic areas of the cortex (Mitrofanis and Mikuletic, 1999; Roger and Cadusseau, 1985), which are known to facilitate and modulate motor behaviour. The ZI sends efferents to the centromedian and parafascicular nuclei (CM/Pf) of the thalamus (Power *et al.*, 1999; Power and Mitrofanis, 2002), the ventral anterior (VA) and ventral lateral (VL) nuclei of the thalamus (Bartho *et al.*, 2002), the mid-brain extrapyramidal area (MEA) (Heise and Mitrofanis, 2004), basal ganglia output nuclei (Heise and Mitrofanis, 2004) and the cortex (Lin *et al.*, 1990; Nicolelis *et al.*, 1995; Lin *et al.*, 1997) (Fig. 7).

The ZI is thought to have several physiological functions. Its rostral sector has been attributed with visceral control (Mok and Mogenson, 1987; Spencer *et al.*, 1988; Tonelli and Chiaraviglio, 1993; Tonelli and Chiaraviglio, 1995), its dorsal

Fig. 7 Schematic diagram showing the key afferent and efferent connections of the zona incerta. Afferent fibres are shown as white arrows, efferent fibres are shown as red arrows. Efferent fibres from CM/Pf to posterodorsal putamen are shown in green. (PUT putamen, GPe globus pallidus externus, GPi globus pallidus internus, SNr substantia nigra reticulata, STN subthalamic nucleus, RAS reticular activating system, MEA midbrain extrapyramidal area, ZI zona incerta, CM/Pf centromedian and parafascicular nucleus of the thalamus, VA/VL ventral anterior and ventral lateral nucleus of the thalamus, MC motor cortex, PMC premotor cortex).

sector with arousal (Berry *et al.*, 1986; Power *et al.*, 2001), its ventral sector with orientating eye/head movements (attention) (May *et al.*, 1997; Shaw and Mitrofanis, 2002), and its caudal sector with the generation of axial and proximal limb movements including locomotion (Mogenson *et al.*, 1985; Milner and Mogenson, 1988; Murer and Pazo, 1993; Perier *et al.*, 2002). Mitrofanis *et al.* have recently speculated that the ZI forms a synaptic interface of the diencephalon, linking diverse sensory inputs (somatic and visceral) to appropriate visceral, arousal, attention and posture locomotion responses (Mitrofanis, 2005).

Abnormal burst firing as well as synchronized oscillations in the 3–7, 13–20, 20–35 Hz (Levy *et al.*, 2000, 2002*a*, *b*; Williams *et al.*, 2002), 60–100 Hz (Trottenberg *et al.*, 2006) and 300 Hz (Foffani *et al.*, 2003) bands have been recorded in the GPi and STN of patients undergoing functional neurosurgery for Parkinson's disease. Oscillations in the beta and gamma frequency bands have been found to be coherent with oscillations simultaneously recorded in the motor cortex (Levy *et al.*, 2000, 2002*a*, *b*; Williams *et al.*, 2002). Brown *et al.* have proposed that the synchronized 13–32 Hz oscillations in the basal ganglia have an antikinetic effect and have shown an inverse relationship with motor function (Brown, 2003; Kuhn *et al.*, 2004), whereas Foffani *et al.* (2005) have shown the presence of these oscillations during movement as well and more recently, immediately after high frequency stimulation of the STN (Foffani *et al.*, 2006).

The 3–7 Hz oscillations have been correlated with the presence of tremor (Nini *et al.*, 1995; Bergman *et al.*, 1998; Raz *et al.*, 2000).

Although unclear, it is likely that these abnormal patterns of neuronal firing will be transmitted to the ZI via afferents from the basal ganglia output nuclei and the motor cortex; and indeed abnormal oscillations with burst firing at 4 and 20 Hz have been recorded in the ZI (Merello *et al.*, 2004). More recently oscillations in the gamma frequency range (60–100 Hz) have also been recorded in this nucleus (Foffani *et al.*, 2006). The ZI will then be in a position to transmit these oscillations via its efferent connections to the thalamic nuclei (CM/Pf and ventral intermedius), the brainstem locomotor centre and back to the basal ganglia output nuclei (GPi and SNr) and the cortex.

We speculate that the effect of transmitting these abnormal patterns of neuronal firing to the CM/Pf nucleus of the thalamus will be to disrupt normal information processing in the striatum and the basal ganglia output nuclei (GPi and SNr) via its efferents to these structures. The ZI's direct connections with the ventral intermediate (Vim) nucleus of the thalamus (Bartho *et al.*, 2002) may be the means by which tremor related oscillations are transmitted to this nucleus, which otherwise receives no direct connections from the basal ganglia output nuclei (GPi and SNr), but receives mainly cerebellar and proprioceptive afferents (Ilinsky and Kultas-Ilinsky, 2002). The abnormal firing patterns transmitted from the cZI to the MEA in Parkinson's disease may also contribute to the impairment of
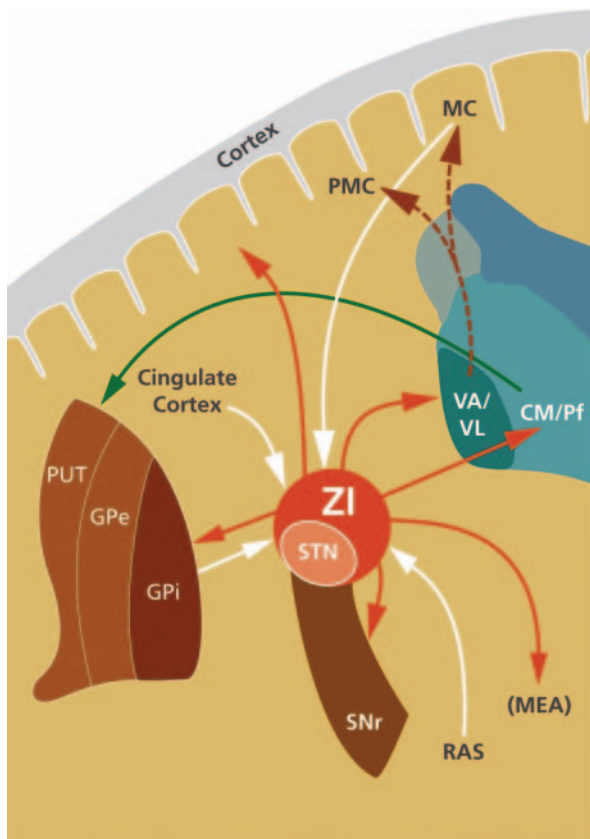
locomotion, axial and gross limb movements seen in this condition.

High frequency stimulation of the cZI in overriding these abnormal oscillations may then have a more profound effect in controlling the symptoms of Parkinson's disease than stimulation of the STN, whose efferents are predominantly confined to the basal ganglia output nuclei and MEA.

Conclusion

This observational study demonstrates that high frequency stimulation of the cZI results in greater improvement in contralateral motor scores in patients with medically refractory Parkinson's disease than stimulation of the STN. These results, if replicated in larger randomized controlled studies, have important implications for our current surgical management of patients with Parkinson's disease and point to a more promising target area for future neurosurgical interventions.

Supplemetary material

Supplementary material is available at *Brain* online.

Acknowledgements

References

Bartho P, Freund TF, Acsady L. Selective GABAergic innervation of thalamic nuclei from zona incerta. Eur J Neurosci 2002; 16: 999–1014.

Bergman H, Raz A, Feingold A, Nini A, Nelken I, Hansel D, et al. Physiology of MPTP tremor. Mov Disord 1998; 13 Suppl 3: 29–34.

Berney A, Vingerhoets F, Perrin A, Guex P, Villemure JG, Burkhard PR, et al. Effect on mood of subthalamic DBS for Parkinson's disease: a consecutive series of 24 patients. Neurology 2002; 59: 1427–9.

Berry DJ, Ohara PT, Jeffery G, Lieberman AR. Are there connections between the thalamic reticular nucleus and the brainstem reticular formation? J Comp Neurol 1986; 243: 347–62.

Binder DK, Rau GM, Starr PA. Risk factors for hemorrhage during microelectrode-guided deep brain stimulator implantation for movement disorders. Neurosurgery 2005; 56: 722–32; discussion.

Brown P. Oscillatory nature of human basal ganglia activity: relationship to the pathophysiology of Parkinson's disease. Mov Disord 2003; 18: 357–63.

Defer GL, Widner H, Marie RM, Remy P, Levivier M. Core assessment program for surgical interventional therapies in Parkinson's disease (CAPSIT-PD). Mov Disord 1999; 14: 572–84.

Foffani G, Priori A, Egidi M, Rampini P, Tamma F, Caputo E, et al. 300-Hz subthalamic oscillations in Parkinson's disease. Brain 2003; 126: 2153–63.

Foffani G, Bianchi AM, Baselli G, Priori A. Movement-related frequency modulation of beta oscillatory activity in the human subthalamic nucleus. J Physiol 2005; 568: 699–711.

Foffani G, Ardolino G, Egidi M, Caputo E, Bossi B, Priori A. Subthalamic oscillatory activities at beta or higher frequency do not change after high-frequency DBS in Parkinson's disease. Brain Res Bull 2006; 69: 123–30.

Figueiras-Mendez R, Regidor I, Riva-Meana C, Magarinos-Ascone CM. Further supporting evidence of beneficial subthalamic stimulation in Parkinson's patients. Neurology 2002; 58: 469–70.

Hamel W, Fietzek U, Morsnowski A, Schrader B, Herzog J, Weinert D, et al. Deep brain stimulation of the subthalamic nucleus in Parkinson's disease: evaluation of active electrode contacts. J Neurol Neurosurg Psychiatry 2003; 74: 1036–46.

Hariz MI, Fodstad H. Do microelectrode techniques increase accuracy or decrease risks in pallidotomy and deep brain stimulation? A critical review of the literature. Stereotact Funct Neurosurg 1999; 72: 157–69.

Heise CE, Mitrofanis J. Evidence for a glutamatergic projection from the zona incerta to the basal ganglia of rats. J Comp Neurol 2004; 468: 482–95.

Herzog J, Fietzek U, Hamel W, Morsnowski A, Steigerwald F, Schrader B, et al. Most effective stimulation site in subthalamic deep brain stimulation for Parkinson's disease. Mov Disord 2004; 19: 1050–4.

Holsheimer J. Principles of neurostimulation. In: Simpson BA, editor. Electrical stimulation and the relief of pain. Vol. 15. Amsterdam: Elsevier; 2003.

Houdart R, Mamo H, Dondey M, Cophignon J. [Results of subthalamic coagulations in Parkinson's disease (apropos of 50 cases)]. Rev Neurol (Paris) 1965; 112: 521–9.

Houeto JL, Mesnage V, Mallet L, Pillon B, Gargiulo M, du Moncel ST, et al. Behavioural disorders, Parkinson's disease and subthalamic stimulation. J Neurol Neurosurg Psychiatry 2002; 72: 701–7.

Hughes AJ, Daniel SE, Kilford L, Lees AJ. Accuracy of clinical diagnosis of idiopathic Parkinson's disease: a clinico-pathological study of 100 cases. J Neurol Neurosurg Psychiatry 1992; 55: 181–4.

Ilinsky IA, Kultas-Ilinsky K. Motor thalamic circuits in primates with emphasis on the area targeted in treatment of movement disorders. Mov Disord 2002; 17 Suppl 3: S9–14.

Ito Z. Stimulation and destruction of the prelemniscal radiation or its adjacent area in various extrapyramidal disorders. Confin Neurol 1975; 37: 41–8.

Jimenez F, Velasco F, Velasco M, Brito F, Morel C, Marquez I, et al. Subthalamic prelemniscal radiation stimulation for the treatment of Parkinson's disease: electrophysiological characterization of the area. Arch Med Res 2000; 31: 270–81.

Jones EG. The thalamus. New York: Plenum Press; 1985.

Kitagawa M, Murata J, Uesugi H, Kikuchi S, Saito H, Tashiro K, et al. Two-year follow-up of chronic stimulation of the posterior subthalamic white matter for tremor-dominant Parkinson's disease. Neurosurgery 2005; 56: 281–9; discussion 281–9.

Kleiner-Fisman G, Fisman DN, Sime E, Saint-Cyr JA, Lozano AM, Lang AE. Long-term follow up of bilateral deep brain stimulation of the subthalamic nucleus in patients with advanced Parkinson disease. J Neurosurg 2003; 99: 489–95.

Kolmac CI, Power BD, Mitrofanis J. Patterns of connections between zona incerta and brainstem in rats. J Comp Neurol 1998; 396: 544–55.

Kosta P, Argyropoulou MI, Markoula S, Konitsiotis S. MRI evaluation of the basal ganglia size and iron content in patients with Parkinson's disease. J Neurol 2006; 253: 26–32.

Krack P, Batir A, Van Blercom N, Chabardes S, Fraix V, Ardouin C, et al. Five-year follow-up of bilateral stimulation of the subthalamic nucleus in advanced Parkinson's disease. N Engl J Med 2003; 349: 1925–34.

Kuhn AA, Williams D, Kupsch A, Limousin P, Hariz M, Schneider GH, et al. Event-related beta desynchronization in human subthalamic nucleus correlates with motor performance. Brain 2004; 127: 735–46.

Kulisevsky J, Berthier ML, Gironell A, Pascual-Sedano B, Molet J, Pares P. Mania following deep brain stimulation for Parkinson's disease. Neurology 2002; 59: 1421–4.

Lanotte MM, Rizzone M, Bergamasco B, Faccani G, Melcarne A, Lopiano L. Deep brain stimulation of the subthalamic nucleus: anatomical and neurophysiological and outcome correlations with the effects of stimulation. J Neurol Neurosurg Psychiatry 2002; 72: 53–8.

Levy R, Hutchison WD, Lozano AM, Dostrovsky JO. High-frequency synchronization of neuronal activity in the subthalamic nucleus of parkinsonian patients with limb tremor. J Neurosci 2000; 20: 7766–75.

Levy R, Ashby P, Hutchison WD, Lang AE, Lozano AM, Dostrovsky JO. Dependence of subthalamic nucleus oscillations on movement, dopamine in Parkinson's disease. Brain 2002a; 125: 1196–209.

Levy R, Hutchison WD, Lozano AM, Dostrovsky JO. Synchronized neuronal discharge in the basal ganglia of parkinsonian patients is limited to oscillatory activity. J Neurosci 2002b; 22: 2855–61.

Limousin P, Krack P, Pollak P, Benazzouz A, Ardouin C, Hoffmann D, et al. Electrical stimulation of the subthalamic nucleus in advanced Parkinson's disease. N Engl J Med 1998; 339: 1105–11.

Lin CS, Nicolelis MA, Schneider JS, Chapin JK. A major direct GABAergic pathway from zona incerta to neocortex. Science 1990; 248: 1553–6.

Lin RC, Nicolelis MA, Chapin JK. Topographic and laminar organizations of the incertocortical pathway in rats. Neuroscience 1997; 81: 641–51.

Littlechild P, Varma TR, Eldridge PR, Fox S, Forster A, Fletcher N, et al. Variability in position of the subthalamic nucleus targeted by magnetic resonance imaging and microelectrode recordings as compared to atlas co-ordinates. Stereotact Funct Neurosurg 2003; 80: 82–7.

May PJ, Sun W, Hall WC. Reciprocal connections between the zona incerta and the pretectum and superior colliculus of the cat. Neuroscience 1997; 77: 1091–114.

Merello M, Tenca E, Cerquetti D. Neuronal activity of the zona incerta in Parkinson's disease patients. Mov Disord 2004; 19: S308.

Milner KL, Mogenson GJ. Electrical and chemical activation of the mesencephalic and subthalamic locomotor regions in freely moving rats. Brain Res 1988; 452: 273–85.

Mitrofanis J. Some certainty for the 'zone of uncertainty'? Exploring the function of the zona incerta Neuroscience 2005; 130: 1–15.

Mitrofanis J, Ashkan K, Wallace BA, Benabid AL. Chemoarchitectonic heterogeneities in the primate zona incerta: Clinical and functional implications. J Neurocytol 2004; 33: 429–40.

Mitrofanis J, Mikuletic L. Organisation of the cortical projection to the zona incerta of the thalamus. J Comp Neurol 1999; 412: 173–85.

Mogenson GJ, Swanson LW, Wu M. Evidence that projections from substantia innominata to zona incerta, mesencephalic locomotor region contribute to locomotor activity. Brain Res 1985; 334: 65–76.

Mok D, Mogenson GJ. Convergence of signals in the zona incerta for angiotensin-mediated and osmotic thirst. Brain Res 1987; 407: 332–40.

Morel A, Magnin M, Jeanmonod D. Multiarchitectonic and stereotactic atlas of the human thalamus. J Comp Neurol 1997; 387: 588–630.

Mundinger F. Stereotaxic interventions on the zona incerta area for treatment of extrapyramidal motor disturbances and their results. Confin Neurol 1965; 26: 222–30.

Murer MG, Pazo JH. Circling behaviour induced by activation of GABAA receptors in the subthalamic nucleus. Neuroreport 1993; 4: 1219–22.

Nicolelis MA, Chapin JK, Lin RC. Development of direct GABAergic projections from the zona incerta to the somatosensory cortex of the rat. Neuroscience 1995; 65: 609–31.

Nini A, Feingold A, Slovin H, Bergman H. Neurons in the globus pallidus do not show correlated activity in the normal monkey, but phase-locked oscillations appear in the MPTP model of parkinsonism. J Neurophysiol 1995; 74: 1800–5.

Ostergaard K, Sunde N, Dupont E. Effects of bilateral stimulation of the subthalamic nucleus in patients with severe Parkinson's disease, motor fluctuations. Mov Disord 2002; 17: 693–700.

Parent A, Hazrati LN. Functional anatomy of the basal ganglia II. The place of subthalamic nucleus and external pallidum in basal ganglia circuitry. Brain Res Brain Res Rev 1995; 20: 128–54.

Patel NK, Heywood P, O'Sullivan K, Love S, Gill SS. MRI-directed subthalamic nucleus surgery for Parkinson's disease. Stereotact Funct Neurosurg 2002; 78: 132–45.

Patel NK, Heywood P, O'Sullivan K, McCarter R, Love S, Gill SS. Unilateral subthalamotomy in the treatment of Parkinson's disease. Brain 2003a; 126: 1136–45.

Patel NK, Plaha P, O'Sullivan K, McCarter R, Heywood P, Gill SS. MRI directed bilateral stimulation of the subthalamic nucleus in patients with Parkinson's disease. J Neurol Neurosurg Psychiatry 2003b; 74: 1631–7.

Perier C, Tremblay L, Feger J, Hirsch EC. Behavioral consequences of bicuculline injection in the subthalamic nucleus and the zona incerta in rat. J Neurosci 2002; 22: 8711–9.

Plaha P, Patel NK, Gill SS. Stimulation of the subthalamic region for essential tremor. J Neurosurg 2004; 101: 48–54.

Power BD, Kolmac CI, Mitrofanis J. Evidence for a large projection from the zona incerta to the dorsal thalamus. J Comp Neurol 1999; 404: 554–65.

Power BD, Leamey CA, Mitrofanis J. Evidence for a visual subsector within the zona incerta. Vis Neurosci 2001; 18: 179–86.

Power BD, Mitrofanis J. Ultrastructure of afferents from the zona incerta to the posterior and parafascicular thalamic nuclei of rats. J Comp Neurol 2002; 451: 33–44.

Raz A, Vaadia E, Bergman H. Firing patterns and correlations of spontaneous discharge of pallidal neurons in the normal and the tremulous 1-methyl-4-phenyl-12,3,6–tetrahydropyridine vervet model of parkinsonism. J Neurosci 2000; 20: 8559–71.

Rezai AR, Phillips M, Baker KB, Sharan AD, Nyenhuis J, Tkach J, et al. Neurostimulation system used for deep brain stimulation (DBS): MR safety issues and implications of failing to follow safety recommendations. Invest Radiol 2004; 39: 300–3.

Richter EO, Hoque T, Halliday W, Lozano AM, Saint-Cyr JA. Determining the position and size of the subthalamic nucleus based on magnetic resonance imaging results in patients with advanced Parkinson disease. J Neurosurg 2004; 100: 541–6.

Rodriguez-Oroz MC, Obeso JA, Lang AE, Houeto JL, Pollak P, Rehncrona S, et al. Bilateral deep brain stimulation in Parkinson's disease: a multicentre study with 4 years follow-up. Brain 2005; 128: 2240–9.

Roger M, Cadusseau J. Afferents to the zona incerta in the rat: a combined retrograde and anterograde study. J Comp Neurol 1985; 241: 480–92.

Saint-Cyr JA, Hoque T, Pereira LC, Dostrovsky JO, Hutchison WD, Mikulis DJ, et al. Localization of clinically effective stimulating electrodes in the human subthalamic nucleus on magnetic resonance imaging. J Neurosurg 2002; 97: 1152–66.

Schaltenbrand G, Bailey P. Introduction to stereotaxis with an atlas of the human brain. Vol. III. Stuttgart: Georg Thieme Verlag; 1959.

Schaltenbrand G, Wahren W. Atlas of stereotaxy of the human brain. Stuttgart: Thieme; 1977.

Shammah-Lagnado SJ, Negrao N, Ricardo JA. Afferent connections of the zona incerta: a horseradish peroxidase study in the rat. Neuroscience 1985; 15: 109–34.

Shaw V, Mitrofanis J. Anatomical evidence for somatotopic maps in the zona incerta of rats. Anat Embryol (Berl) 2002; 206: 119–30.

Spencer SE, Sawyer WB, Loewy AD. L-glutamate stimulation of the zona incerta in the rat decreases heart rate and blood pressure. Brain Res 1988; 458: 72–81.

Tonelli L, Chiaraviglio E. Enhancement of water intake in rats after lidocaine injection in the zona incerta. Brain Res Bull 1993; 31: 1–5.

Tonelli L, Chiaraviglio E. Dopaminergic neurons in the zona incerta modulates ingestive behavior in rats. Physiol Behav 1995; 58: 725–9.

Trottenberg T, Fogelson N, Kuhn AA, Kivi A, Kupsch A, Schneider GH, et al. Subthalamic gamma activity in patients with Parkinson's disease. Exp Neurol, 2006 [Epub ahead of print].

Velasco F, Jimenez F, Perez ML, Carrillo-Ruiz JD, Velasco AL, Ceballos J, et al. Electrical stimulation of the prelemniscal radiation in the treatment of Parkinson's disease: an old target revised with new techniques. Neurosurgery 2001; 49: 293–306; discussion 306–8.

Voges J, Volkmann J, Allert N, Lehrke R, Koulousakis A, Freund HJ, et al. Bilateral high-frequency stimulation in the subthalamic nucleus for the treatment of Parkinson disease: correlation of therapeutic effect with anatomical electrode position. J Neurosurg 2002; 96: 269–79.

Volkmann J, Allert N, Voges J, Weiss PH, Freund HJ, Sturm V. Safety, efficacy of pallidal or subthalamic nucleus stimulation in advanced PD. Neurology 2001; 56: 548–51.

Watanabe K, Kawana E. The cells of origin of the incertofugal projections to the tectum, thalamus, tegmentum and spinal cord in the rat: a study using the autoradiographic and horseradish peroxidase methods. Neuroscience 1982; 7: 2389–406.

Williams D, Tijssen M, Van Bruggen G, Bosch A, Insola A, Di Lazzaro V, et al. Dopamine-dependent changes in the functional connectivity between basal ganglia and cerebral cortex in humans. Brain 2002; 125: 1558–69.

Yelnik J, Damier P, Demeret S, Gervais D, Bardinet E, Bejjani BP, et al. Localization of stimulating electrodes in patients with Parkinson disease by using a three-dimensional atlas-magnetic resonance imaging coregistration method. J Neurosurg 2003; 99: 89–99.

Yelnik J, Percheron G. Subthalamic neurons in primates: a quantitative, comparative analysis. Neuroscience 1979; 4: 1717–43.

Yokoyama T, Sugiyama K, Nishizawa S, Yokota N, Ohta S, Akamine S, et al. The optimal stimulation site for chronic stimulation of the subthalamic nucleus in Parkinson's disease. Stereotact Funct Neurosurg 2001; 77: 61–7.

Zonenshayn M, Sterio D, Kelly PJ, Rezai AR, Beric A. Location of the active contact within the subthalamic nucleus (STN) in the treatment of idiopathic Parkinson's disease. Surg Neurol 2004; 62: 216–25; discussion 225–6.